RSC Advances

ROYAL SOCIETY OF CHEMISTRY

www.rsc.org/advances

Journal Name

RSCPublishing

Paper

Synthesis, Characterization of Gold Complexes with Pyridine-based SNS Ligands and as Homogeneous Catalysts for Reduction of 4-Nitrophenol

Wei-Guo Jia*, Yuan-Chen Dai, Hai-Ning Zhang, XiaoJing Lu, En-Hong Sheng

Cite this: DOI: 10.1039/x0xx00000x

Received 00th January 2012,
Accepted 00th January 2012

DOI: 10.1039/x0xx00000x

www.rsc.org/

Three gold complexes with pyridine-based SNS type ligands, 2,6-bis(1-methylimidazole-2-thione)pyridine (**Bmtp**), 2,6-bis(1-ethylimidazole-2-thione)pyridine (**Betp**) and 2,6-bis(1-isopropylimidazole-2-thione)pyridine (**Bptp**) have been synthesized and characterized. Reactions of $HAuCl_4 \cdot H_2O$ with three pyridine-based SNS ligands result in the formation of the complexes $[(L)AuCl_2]Cl$ (L = **Bmtp** (**1**); L = **Betp** (**2**) and L = **Bptp** (**3**)), respectively. All compounds are investigated by elemental analysis, NMR, MS and UV-Vis as well as IR spectra analysis. The molecular structure of **3** has been confirmed by X-ray crystallography. Moreover, all gold complexes as homogeneous catalysts are efficiently catalyze 4-nitrophenol (4-NP) reduction to 4-nitroaniline (4-AP) in the presence of $NaBH_4$ reducing agent in water. And the complex **3** exhibits an exceptionally high turn over frequency (TOF) of 1.20 min^{-1} for reduction of 4-NP.

Introduction

Gold-based compounds including complexes and nanomaterials (particles, box, cage and tube) exhibit extraordinarily rich catalytic activity for a variety of reactions involving oxidation and reduction due to their unique physicochemical properties in the past few decades.[1, 2] The interest of exploring gold-based catalysts has been substantially booming. For heterogeneous gold-based catalytic system, a high dispersion of gold nanoparticles is necessary to exhibit high catalytic activity. Then, many solid supporting gold catalysts including polymer,[3] hydrogel,[4] silica particles,[5] metal oxides [6] and magnetic materials [7] have been developed.[2] In contrast to the heterogeneous catalytic system, homogeneous gold catalysts have been found to be very effective for construction of C-C, C-N bond through C-H activation.[8] The mechanisms of the heterogeneous reactions are not yet well understand, whereas the mechanisms have been well explored in the case of the homogeneous reactions are possible. Therefore, the design and synthesis of homogeneous gold catalysts with stable and high catalytic efficiency have received increasing attention recently.

In previous studies, we synthesized Ir and Rh complexes based on organochalcogen ligands (SS, SeSe and SNS) and studied their catalytic activities in norbornene polymerization.[9, 10] Orchanochalcogen chemistry revolving transition metal complexes is one of research focuses of our groups, and we seek to discover new transition metal complexes and study their potential catalytic applications. Herein, the gold complexes with three pyridine-based SNS ligands $[(L)AuCl_2]Cl$ (L = **Bmtp** (**1**); L = **Betp** (**2**) and L = **Bptp** (**3**)) have been synthesized and characterized. Moreover, the molecular structure of **3** has been determined by X-ray crystallography. The various organochalcogen ligands were selected in order to investigate the influence of alkyl substituents on imidazole ring with different electronic properties on catalytic properties of the resulting complexes. The results show that all gold complexes are efficiently catalyze 4-NP reduction to 4-AP in the presence of $NaBH_4$ reducing agent under homogeneous conditions. Furthermore, the steric and electronic effects of the alkyl group in the organochalcogen ligands have a strong influence on the 4-NP reduction (*i*-Pr > Et > Me).

Results and discussion

Synthesis of ligands and gold complexes

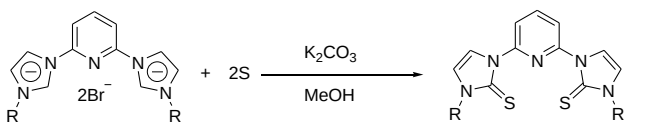

Scheme 1. Synthesis of pyridine-based SNS ligands

Three pyridine-based SNS ligands, 2,6-bis(1-methylimidazole-2-thione)pyridine (**Bmtp**), 2,6-bis(1-ethylimidazole-2-thione)pyridine (**Betp**) and 2,6-bis(1-isopropylimidazole-2-

thione)pyridine (**Bptp**) were prepared in one-pot *via* the reactions of pyridine bridged imidazolium dibromide derivatives with sulfur powder in the presence of K_2CO_3 according to the previous literature method (**Scheme 1**).[10, 11] All these compounds were stable towards air and moisture in the solid state, and exhibit good solubility in common organic solvents. All compounds were characterized by NMR, IR spectroscopy as well as elemental analysis. The ^{1}H NMR spectrum of **Betp** show signals at δ 1.42, 4.18, 6.82, 7.49, 8.02 and 8.88 ppm, which can be assigned to the alkyl, imidazole, and pyridyl groups, respectively. And the ^{13}C NMR spectra show singlet at about δ 161.8 ppm for C=S group in **Betp**, which is also consistent with **Bmtp** and **Bptp**.

When $HAuCl_4$ was treated with three pyridine-based SNS ligands: **Bmtp**, **Betp** and **Bptp** in MeOH at room temperature, the orange crystals of gold complexes (**1-3**) were isolated in moderate yields as air and moisture-stable, respectively (**Scheme 2**). Complexes **1-3** were fully characterized by IR, NMR spectroscopy, elemental analysis as well as MS. All these gold complexes have similar characteristic peaks on NMR spectra, so it is feasible to take **1** for an example. The ^{1}H NMR spectrum of **1** show signals at δ 4.13, 7.75, 7.85, 7.94 and 8.47 ppm, which can be assigned to the methyl, imidazole, and pyridyl groups, respectively. Likewise, upfield shifts of up to 15.4 ppm for the thione carbons in their ^{13}C NMR were measured upon complexation to gold metal, which also prove the formation of the gold complex.

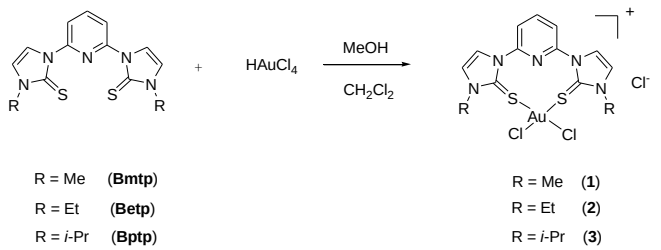

Scheme 2. Synthesis of gold complexes (**1-3**) with pyridine-based SNS ligands

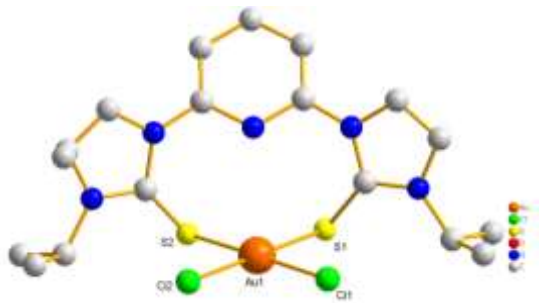

Fig. 1 Crystal structure of [(**Bptp**)$AuCl_2$]$^+$ anion, hydrogen atoms are omitted for clarity.

Crystals of **3** suitable for X-ray crystallographic diffraction were obtained by slow diffusion of diethyl ether into a concentrated solution of the complex in methanol solution.

Table 1 Crystallographic data and structure refinement parameters for gold complex **3**

	3
Empirical formula	$C_{18}H_{21}AuCl_3N_5O_2S_2$
Formula weight	706.830
Crystal syst., Space group	Triclinic, P-1
a (Å)	7.981(4)
b (Å)	11.981(6)
c (Å)	15.652(8)
α (°)	106.507(6)
β (°)	104.098(6)
γ (°)	97.096(6)
Volume (Å^3), Z	1361.5(12), 2
D_c (mg / m^3)	1.724
μ (Mo-Kα) (mm^{-1})	5.873
F(000)	684
θ range (°)	1.81 ~ 27.62
Limiting indices	-10, 10; -15, 14; -20, 20
Reflections/unique[R(int)]	6033/2740 [0.0988]
Completeness to θ (°)	27.62 (95.2 %)
Data/restraints/parameters	6033 / 0 / 243
Goodness-of-fit on F^2	0.956
Final *R* indices [I > 2σ(I)][a]	R_1= 0.0797, wR_2= 0.1770
R indices (all data)	R_1= 0.1977, wR_2= 0.2250

[a] $R_1 = \Sigma||F_o|-|F_c||/\Sigma|F_o|$; $wR_2 = [\Sigma w(|F_o^2|-|F_c^2|)^2/\Sigma w|F_o^2|^2]^{1/2}$.

Table 2 Selected bond lengths (Å) and bond angles (°) for gold complex **3**

Au1-S1	2.340(5)	Au1-S2	2.332(4)
Au1-Cl1	2.320(4)	Au1-Cl2	2.315(5)
S1-Au1-S2	88.86(15)	S1-Au1-Cl1	90.10(17)
S1-Au1-Cl2	178.51(17)	S2-Au1-Cl1	178.08(19)
S2-Au1-Cl2	89.80(16)	Cl1-Au1-Cl2	91.22(18)

Crystallographic data and details of data collection and refinement for complex **3** are summarized in **Table 1**, the important bond lengths and angles are given in **Table 2**. The molecular structure of **3** is shown in **Fig. 1**.

The molecular structure of **3** is solved in the triclinic crystal system and *P-1* space group. As can be seen, the coordination geometry of the central gold center can be best described as a nearly square-planar geometry with two Cl atoms and two N atoms (S1-Au1-S2 88.86(15)°, S1-Au1-Cl1 90.10(17)°, S1-Au1-Cl2 178.51(17)°, S2-Au1-Cl1 178.08(19)°, S2-Au1-Cl2 89.80(16)° and Cl1-Au1-Cl2 91.22(18). Both sulfur atoms and two chlorine atoms of **Bptp** ligand in a *cis* disposition. Bond distances around the gold ion are as expected (Au-Cl_{av} = 2.318 Å and Au-S_{av} = 2.336 Å) and are comparable to the distances observed in the [$AuCl_2(S_2CNBn_2)$] (Au-Cl = 2.3116(15) Å, Au-S = 2.3005(14) Å).[12]

As shown in the **Fig. 2**, in complex **3**, there are two kinds of weak intermolecular C-H···Cl hydrogen bonds between chlorine anion and carbon of ligand. One is C-H···Cl hydrogen bond (C(4)-C1(3) = 3.49(2) Å, C(4)-H(4)···Cl(3) = 169°) and the other is C-H···Cl hydrogen bond (C(13)-C1(3) = 3.484(14) Å, C(13)-H(13)···Cl(3) = 174°). These weak intramolecular hydrogen bonds play a crucial role in the construction of 1D polymeric chain structure in the solid states. And the similar weak interactions have been found among the transition metal coordination complexes.[13]

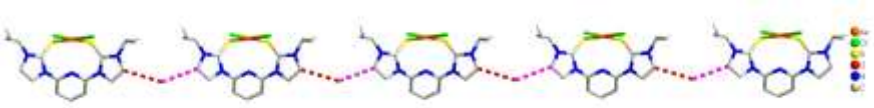

Fig. 2 View of 1D intertwined supramolecular polymeric chains in **3**

Catalytic degradation of 4-NP

Catalytic reduction of 4-NP is possibly the most often used reaction to test the catalytic activity of gold-based catalysts in aqueous solution.[14] 4-NP is one of the most common organic pollutants found in dye industrial and agricultural wastewaters. The reduction of 4-NP by gold-based catalysts in the presence of $NaBH_4$ reducing agent leads to the formation of 4-AP, which is an useful compound for a wide range of applications include pharmaceuticals, corrosion treatments, and so on.[15] The catalytic performance of the gold complexes were evaluated in the reduction of 4-NP in the presence of $NaBH_4$ under homogeneous conditions in water. The catalytic reactions were monitored by UV-Vis spectroscopy, by recording the UV spectra of aliquots withdrawn from the reaction medium at 1 min intervals. In **Fig. 3** are presented the time-dependent UV-Vis spectra of the 4-NP reduction catalyzed by gold complexes catalysts. As shown in **Fig. 3**, upon the increase of the reaction time, the intensity of the absorption band at $\lambda = 400$ nm from 4-nitrophenolate ion becomes weaker, and at the same time, an absorption band around $\lambda = 300$ nm appears due to the formation of 4-AP, which increases in intensity during the course of the reaction.

Fig. 3 A-C provides the time-dependent UV-vis adsorption spectra of the reaction mixture catalyzed by gold complexes. All gold catalysts are highly active in the 4-NP reduction, with the reaction catalyzed by complex **1** reaching the maximum substrate conversion of 93.2% within 13 minutes, whereas for the reaction catalyzed by complex **2** and **3** the maximum conversion of 97.5% and 96.5% were achieved after 11 and 8 minutes of reaction time, respectively. Since the concentration of $NaBH_4$ is much higher than that of 4-NP (100-fold times, See supporting information), the rate of reduction of 4-AP is independent of the $NaBH_4$ concentration which allows this reaction to be evaluated by pseudo-first-order kinetics. The kinetic profiles of the 4-NP reduction using all gold catalysts are presented in **Fig. 3**(D), through the representation of $\ln(C_t/C_0)$ as a function of the reaction time, where C_t and C_0 are the concentration of 4-NP at the beginning and at a certain reaction time respectively. **Fig. 3**(D) shows the $\ln(C_t/C_0)$ versus time for all gold catalysts systems and good linear relationships are observed, indicating that the reduction of 4-NP to 4-AP follows the pseudo-first-order kinetics. The kinetic reaction rate constants (k) were determined from the slope of the straight line which is 2.6×10^{-3} S^{-1} for complex **1**, 2.7×10^{-3} S^{-1} for complex **2** and 5.1×10^{-3} S^{-1} for complex **3**, respectively. This result means that complex **3** possess the faster reduction rate and thus higher catalytic activity for the reduction of 4-NP, which should be attributed to

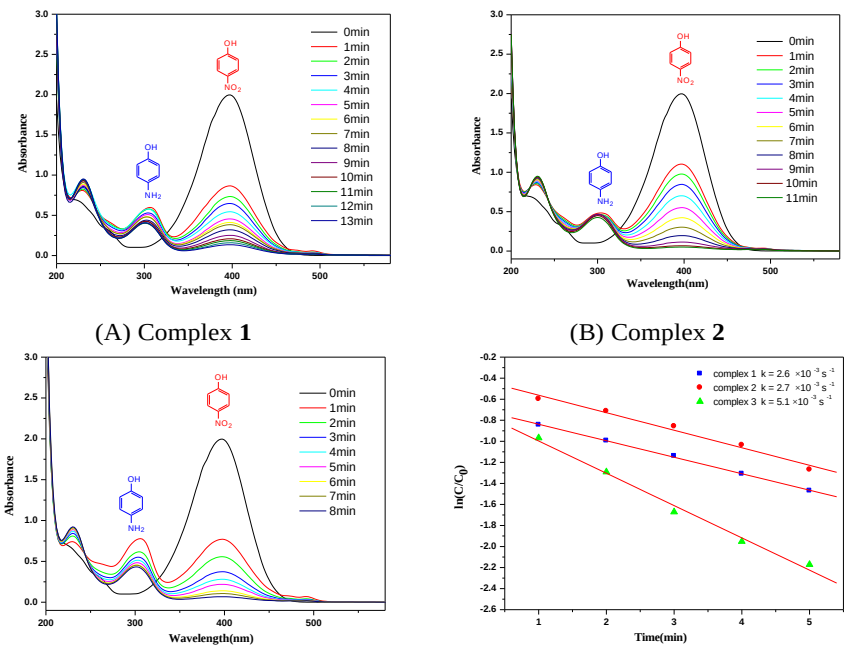

(A) Complex **1** (B) Complex **2**

(C) Complex **3** (D)

Fig. 3 UV-vis adsorption spectra of the reduction of 4-NP by $NaBH_4$ in the presence of gold complexes (A), complex **1** (B), complex **2** (C), complex **3** (D) plot of $\ln(C_t/C_0)$ of 4-NP against time for the catalysts.

the size and electronic effect of alkyl substituent on imidazole ring in gold complexes (*i*-Pr > Et > Me).

In order to evaluate the catalytic results, we use the turnover frequency (TOF) to determine the efficiency of our gold complexes catalysts for 4-NP reduction and compare with previously reported gold based catalysts. The TOF of complex **3** catalyst is 1.20 min^{-1}, calculated by the moles of 4-NP reduced per mole of gold complex per consumed time under the present reaction conditions. As shown in **Table 3**, in comparison with other gold-based catalysts, our gold complexes catalysts showed a higher catalytic efficiency than most of other gold-based catalysts for the reduction of 4-NP. The above results showed that gold complexes with pyridine-based SNS ligands possessed superior high catalytic activity, which should be attributed to the homogeneous catalytic system.

Table 3 Comparison of catalytic activity by Au based catalysts for the reduction of 4-NP

Catalysts	TOF (min^{-1})	Catalysts (mol%)	References
Complex **1**	0.71	10	This work
Complex **2**	0.88	10	This work
Complex **3**	1.20	10	This work
Au(0)@TpPa-1	0.17	45	16
$HAuCl_4 \cdot 3H_2O$	0.11	46	16
Au-PMMA	1.53	7	17
Fe_3O_4@SiO_2-Au@mSiO_2	0.73	9	18
Fe_3O_4@P(EGDMA-co-MAA)/Au	1.6	2.5	19
Au NPs/SNTs	0.77	28	20
PDEAEMA-AuNP	0.47	57	21
Au@SiO_2	0.45	7	22

The UV-vis absorbance of gold complexes

The absorption spectra of all gold complexes and ligands measured at room temperature in MeOH solvents were given in **Fig. 4**. All ligands and gold complexes show intense absorptions at 208 nm which can be assigned to π-π* of pyridine-based SNS ligand. The peaks at 225 and 321 nm were found to become weak in gold complexes, which may be attributed to the charge transfer between pyridine-based SNS ligand and Au(III) metal centre.

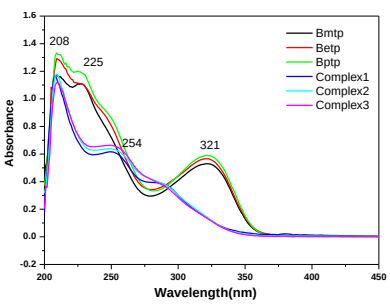

Fig. 4 The UV-vis absorption of gold complexes (1×10^{-4} mol/L) in MeOH.

Conclusion

In conclusion, we have reported three gold complexes with pyridine-based ligands. A combination of spectroscopic studies and X-ray crystallographic confirmed the molecular structures of gold complexes. And all gold complexes are hightly catalyze 4-NP reduction to 4-AP in the presence of $NaBH_4$ reducing agent under homogeneous conditions in water. And the complex **3** exhibits an exceptionally high turn TOF of 1.20 min^{-1} for reduction of 4-NP.

Experimental Section

General: All manipulations were carried out under nitrogen using standard schlenk and vacuum-line techniques. All solvents were purified and degassed by standard procedures. The starting materials, **Bmtp** and **Bptp** were synthesized according to the procedures described in the literature.[10, 11] Other chemicals were analytical grade and used as received. ^1H and ^{13}C NMR were recorded on a 300 MHz or 500 MHz NMR spectrometer at room temperature. Chemical shifts (δ) are given in ppm relative to internal TMS and are internally referenced to residual ^1H and ^{13}C solvent resonances. IR spectra were recorded on a Niclolet AVATAR-360IR spectrometer. Element analyses were performed on an Elementar III vario EI Analyzer. Mass spectrometry was performed on Bruker BIFLEX III MALDI-TOF-MS instrument.

Synthesis of betp

In a 100 mL round-bottomed flask fitted with reflux condenser were placed 2,6-bis(1-ethylimidazolium)pyridine dibromide (3.31 g, 10 mmol), S (0.64 g, 20 mmol), K_2CO_3 (2.8 g, 20 mmol) and 50 mL methanol as solvent. The mixture was allowed to reflux for 8 h after which the methanol was removed with a rotary evaporator. The remaining solid was shaken with 2 × 30 mL CH_2Cl_2 which was then filtered and rotary evaporated. The product was recrystallized from CH_2Cl_2/MeOH to give colorless solid. Yield: (1.92 g 58%) Anal. Calcd. for $C_{15}H_{17}N_5S_2$ (331.09): C, 54.37; H, 5.17; N, 21.15. Found: C, 54.30; H, 5.25; N, 21.30. ^1H NMR (500 MHz $CDCl_3$): 8.88 (d, J = 8 Hz, pyridine, 2H), 8.02 (t, pyridine, 1H), 7.49 (d, J = 3 Hz, imidazole, 2H), 6.82 (d, J = 3 Hz, imidazole, 2H), 4.18 (m, $2CH_2$ 4H), 1.42 (t, $2CH_3$, 6H) ppm. ^{13}C NMR (500 MHz, $CDCl_3$): δ 161.8, 148.4, 139.7, 117.0, 116.3, 116.8, δ 42.7, 13.9 ppm. IR (KBr cm^{-1}): 1143 (m) (C=S).

Synthesis of complex 1

In a 100 mL round-bottomed flask were placed **Bmtp** (152 mg, 0.5 mmol), $HAuCl_4$ (206 mg, 0.5 mmol), 30 mL methanol as solvent. The mixture was stirred at room temperature overnight and then the solvent was removed with a rotary evaporator; the resulting solid was washed with methanol, and then dried in vacuo. The product was recrystallized from MeOH/hexane to give orange powder. Yield: (137 mg, 45%). Anal. Calc. for $C_{13}H_{13}Cl_3N_5S_2Au$ (606.73): C, 25.79; H, 2.17; N, 11.57. Found: C, 25.90; H, 2.28; N, 11.66. ^1H NMR (300 MHz, CD_3CN) δ 8.47 (t, pyridine, 1H), 7.94 (d, J = 2.1 Hz,

imidazole, 2H), 7.85-7.87 (d, pyridine, 2H), 7.75 (d, J = 2.1 Hz, imidazole, 2H), 4.13 (s, 6H). ^{13}C NMR (500 MHz, CD_3CN) δ 147.54, 144.90, 125.90, 123.95, 121.80, 30.29. MS (MALDI-TOF): calcd. for $C_{13}H_{13}N_5S_2Au^{3+}$ 500.0278 (M^{3+}), found 500.1567 (M^{3+}). IR (KBr cm^{-1}): 3451 (m), 3136 (w), 3114 (w), 3077 (w), 1595 (m), 1551 (w), 1477 (s), 1400 (w), 1317 (w), 1239 (m), 1165 (w), 1087 (w), 999 (w), 819 (m), 767 (w), 748 (m), 718 (w), 680 (w), 615 (w), 543 (w).

Synthesis of complex 2

A procedure similar to that used for the preparation of **1** was employed. Yield: 159 mg, 50%). Anal. Calc. for $C_{15}H_{17}Cl_3N_5S_2Au$ (632.97): C, 28.44; H, 2.71; N, 11.06. Found: C, 28.56; H, 2.88; N, 11.00. ^{1}H NMR (500 MHz, CD_3OD) δ 8.53 (t, pyridine, 1H), 8.27 (d, J = 2 Hz, imidazole, 2H), 8.10 (d, J = 2 Hz, imidazole, 2H), 8.01 (d, pyridine, 2H), 4.56-4.74 (m, 2H, CH_2), 1.60 (t, 6H).^{13}C NMR (500 MHz, CD_3OD) δ 147.71, 144.49, 143.74, 124.16, 123.89, 121.28, 46.32, 14.33. MS (MALDI-TOF): calcd. for $C_{15}H_{17}N_5S_2Au^{3+}$ 528.0591 (M^{3+}), found 528.2131 (M^{3+}). IR (KBr cm^{-1}): 3410 (m), 3127 (w), 3087 (w), 2978 (w), 2935 (w), 1597 (s), 1473 (s), 1455 (s), 1381 (w), 1347 (w), 1313 (w), 1270 (m), 1222 (m), 1167 (w), 1091 (w), 1050 (w), 815 (w), 775 (w), 753 (w), 733 (w), 703 (w), 675 (w).

Synthesis of complex 3

A procedure similar to that used for the preparation of **1** was employed. Yield: (199 mg, 60%). Anal. Calc. for $C_{17}H_{21}Cl_3N_5S_2Au$ (662.83): C, 30.86; H, 3.20; N, 10.59. Found: C, 30.75; H, 3.18; N, 11.06. ^{1}H NMR (500 MHz, CD_3OD) δ 8.53 (t, pyridine, 1H), 8.29 (d, J = 2 Hz, imidazole, 2H), 8.18 (d, J = 2 Hz, imidazole, 2H), 8.01 (d, pyridine, 2H), 5.51 (m, CH, 2H), 1.74 (d, CH_3, 6H), 1.51 (d, CH_3, 6H).^{13}C NMR (500 MHz, CD_3OD) δ 147.65, 144.45, 142.90, 124.54, 121.38, 53.61, 22.70, 21.17. MS (MALDI-TOF): calcd. for $C_{17}H_{21}N_5S_2Au^{3+}$ 556.0904 (M^{3+}), found 556.3727 (M^{3+}). IR (KBr cm^{-1}): 3408 (m), 3033 (w), 2976 (w), 1598 (m), 1550 (w), 1458 (s), 1404 (w), 1375 (w), 1345 (w), 1312 (w), 1228 (m), 1171 (w), 1076 (w), 996 (w), 960 (w), 881 (w), 811 (w), 755 (w), 729 (w), 695 (w), 633 (w).

Catalytic reduction of 4-NP

The catalytic reduction of 4-NP to 4-AP was carried out at room temperature on a quartz optical cell by monitoring the electronic spectra at 1 min intervals. The degradation of 4-NP was monitored by the absorbance decrease of the electronic band at λ = 400 nm due to nitrophenolate ion in basic media and development of a new electronic band at λ = 300 nm corresponding to the formation of 4-AP. A stock solution of 4-NP (3×10^{-4} mol/L) was prepared. For the study of reduction kinetics, 1 mL of 4-NP stock solution were transferred to the UV-Vis cell and 1.13 mg of $NaBH_4$ (1 ml, 3×10^{-5} mol) were added. Upon addition of the reducing agent, the band at λ = 400 nm remained unaltered until addition of the gold catalyst (1 ml, 3×10^{-8} mol). In this case, the electronic spectra of the reaction mixtures were acquired at each 1 min by withdrawing 3 mL aliquots from the reaction medium.

X-ray Structure Determination.

Diffraction data of **3** was collected on a Bruker AXS SMART APEX diffractometer, equipped with a CCD area detector using Mo Kα radiation (λ = 0.71073 Å). All the data were collected at 298K and the structures were solved by direct methods and subsequently refined on F^2 by using full-matrix least-squares techniques (SHELXL),[23] SADABS[24] absorption corrections were applied to the data, all non-hydrogen atoms were refined anisotropically, and hydrogen atoms were located at calculated positions. All calculations were performed using the Bruker Smart program.

Acknowledgment

We acknowledges financial support from the National Nature Science Foundation of China (21102004), and the Natural Science Foundation of the Anhui Higher Education Institutions of China (KJ2011A146), the Project-sponsored by SRF for ROCS and Special and Excellent Research Fund of Anhui Normal University, National Training Programs of Innovation and Entrepreneurship for Undergraduates (201410370040). Training Programs of Innovation and Entrepreneurship of Anhui Province for Undergraduates (AH201410370040).

Notes and references

College of Chemistry and Materials Science, Center for Nano Science and Technology, The Key Laboratory of Functional Molecular Solids, Ministry of Education, Anhui Laboratory of Molecular-Based Materials, Anhui Normal University, Wuhu, 241000, China
wgjiasy@mail.ahnu.edu.cn (W. -G. Jia)

† Electronic Supplementary Information (ESI) available: CCDC 1044349 crystallographic information files (CIFs) for complex **3** are available, See DOI: 10.1039/

1 (a) A. S. K. Hashmi and G. J. Hutchings, *Angew. Chem. Int. Ed.*, 2006, **45**, 7896-7936; (b) A. S. K. Hashmi, *Chem. Rev.*, 2007, **107**, 3180-3211; (c) J. Zeng, Q. Zhang, J. Chen and Y. Xia, *Nano Lett.*, 2009, **10**, 30-35; (d) J. Oliver-Meseguer, J. R. Cabrero-Antonino, I. Dominguez, A. Leyva-Perez and A. Corma, *Science*, 2012, **338**, 1452-1455; (e) C. Della Pina, E. Falletta, L. Prati and M. Rossi, *Chem. Soc. Rev.*, 2008, **37**, 2077-2095; (f) Y.-F. Han, G.-X. Jin and F. E. Hahn, *J. Am. Chem. Soc.*, 2013, **135**, 9263-9266.

2 A. Corma and H. Garcia, *Chem. Soc. Rev.*, 2008, **37**, 2096-2126.

3 (a) W. Wang, A. Zheng, P. Zhao, C. Xia and F. Li, *ACS Catal.*, 2013, **4**, 321-327; (b) S. Wu, J. Dzubiella, J. Kaiser, M. Drechsler, X. Guo, M. Ballauff and Y. Lu, *Angew. Chem. Int. Ed.*, 2012, **51**, 2229-2233.

4 J. Li, C.-y. Liu and Y. Liu, *J. Mater. Chem.*, 2012, **22**, 8426-8430.

5 V. A. Solovyeva, K. B. Vu, Z. Merican, R. Sougrat and V. O. Rodionov, *ACS Comb. Sci.*, 2014, **16**, 513-517.

6 X. Lv, Y. Zhu, H. Jiang, H. Zhong, X. Yang and C. Li, *Dalton Trans.*, 2014, **43**, 15111-15118.

7 M. Rocha, C. Fernandes, C. Pereira, S. L. H. Rebelo, M. F. R. Pereira and C. Freire, *RSC Adv.*, 2015, **5**, 5131-5141.

8 (a) J. Xie, C. Pan, A. Abdukader and C. Zhu, *Chem. Soc. Rev.*, 2014, **43**, 5245-5256; (b) T. C. Boorman and I. Larrosa, *Chem. Soc. Rev.*, 2011, **40**, 1910-1925.
9 (a) W.-G. Jia, Y.-B. Huang, Y.-J. Lin and G.-X. Jin, *Dalton Trans.*, 2008, 5612-5620; (b) W.-G. Jia, Y.-B. Huang and G.-X. Jin, *J. Organomet. Chem.*, 2009, **694**, 3376-3380.
10 W.-G. Jia, Y.-B. Huang and G.-X. Jin, *J. Organomet. Chem.*, 2009, **694**, 4008-4013.
11 Y.-F. Han, L. Zhang, L.-H. Weng and G.-X. Jin, *J. Am. Chem. Soc.*, 2014, **136**, 14608-14615.
12 J. Cordón, G. Jiménez-Osés, J. M. López-de-Luzuriaga, M. Monge, M. E. Olmos and D. Pascual, *Organometallics*, 2014, **33**, 3823-3830.
13 (a) G. Yuan, Y. Huo, X. Nie, H. Jiang, B. Liu, X. Fang and F. Zhao, *Dalton Trans.*, 2013, **42**, 2921-2929; (b) G. Yuan, L. Rong, X. Qiao, L. Ma and X. Wei, *CrystEngComm*, 2013, **15**, 7307-7314; (c) W.-G. Jia, D.-D. Li, L.-Q. Yan, E.-H. Sheng and Y.-C. Dai, *J. Coord. Chem.*, 2014, **67**, 363-371; (d) Y.-F. Han, Y. Fei and G.-X. Jin, *Dalton Trans.*, 2010, **39**, 3976-3984; (e) Y.-F. Han and G.-X. Jin, *Chem. Soc. Rev.*, 2014, **43**, 2799-2823; (f) Y.-F. Han, Y.-J. Lin and G.-X. Jin, *Dalton Trans.*, 2011, **40**, 10370-10375; (g) Y.-F. Han, H. Li and G.-X. Jin, *Chem. Commun.*, 2010, **46**, 6879-6890; (h) Y.-F. Han, H. Li, Y. Fei, Y.-J. Lin, W.-Z. Zhang and G.-X. Jin, *Dalton Trans.*, 2010, **39**, 7119-7124.
14 P. Herves, M. Perez-Lorenzo, L. M. Liz-Marzan, J. Dzubiella, Y. Lu and M. Ballauff, *Chem. Soc. Rev.*, 2012, **41**, 5577-5587.
15 M. J. Vaidya, S. M. Kulkarni and R. V. Chaudhari, *Org. Process Res. Dev.*, 2003, **7**, 202-208.
16 P. Pachfule, S. Kandambeth, D. Diaz Diaz and R. Banerjee, *Chem. Commun.*, 2014, **50**, 3169-3172.
17 K. Kuroda, T. Ishida and M. Haruta, *J. Mol. Catal. A: Chem.*, 2009, **298**, 7-11.
18 Y. Deng, Y. Cai, Z. Sun, J. Liu, C. Liu, J. Wei, W. Li, C. Liu, Y. Wang and D. Zhao, *J. Am. Chem. Soc.*, 2010, **132**, 8466-8473.
19 H. Woo and K. H. Park, *Catal. Commun.*, 2014, **46**, 133-137.
20 Z. Zhang, C. Shao, P. Zou, P. Zhang, M. Zhang, J. Mu, Z. Guo, X. Li, C. Wang and Y. Liu, *Chem. Commun.*, 2011, **47**, 3906-3908.
21 J. Zhang, D. Han, H. Zhang, M. Chaker, Y. Zhao and D. Ma, *Chem. Commun.*, 2012, **48**, 11510-11512.
22 Z. Wang, H. Fu, D. Han and F. Gu, *J. Mater. Chem. A*, 2014, **2**, 20374-20381.
23 G. Sheldrick, *University of Göttingen, Germany*, 1997.
24 G. Sheldrick, *Bruker AXS, Madison, WI, USA*, 1998.

Table of Content

Three gold complexes are efficiently catalyze 4-nitrophenol reduction to 4-nitroaniline in the presence of $NaBH_4$ under homogeneous conditions in water.